Electronic Structure of Metal/Molecule//Metal Junctions: A Density Functional Theory Study of the Influence of the Molecular Terminal Group†

Q. Sun,‡ A. Selloni,*,‡ and G. Scoles‡,§

Chemistry Department, Princeton University, Princeton, New Jersey 08540, and International School for Advanced Studies and Elettra Synchrotron Labs, Trieste, Italy

Received: July 5, 2005; In Final Form: October 3, 2005

We report on density functional theory calculations of the electronic structure of Au(111)/molecule//Au(111) junctions in which thiol molecules are chemically bound at one end to a gold electrode (the "substrate"), while the other end has a separation of a few to several angstroms from a second gold electrode (the "tip"). Our goal is to investigate the role of different molecular terminal groups and of the tip−molecule distance either on the spatial dependence of the local density of states (LDOS) at the Fermi energy E_f or on the energy dependence of the projected density of states onto different molecular subunits. We consider conjugated diphenylthiol (SPh2R) molecules with terminal groups R = H, SH, CH_3, or CF_3 as well as "mixed" conjugated−saturated phenylthiol-pentane ($SPhC4CH_3$) and butanethiol-toluene ($SC4PhCH_3$) molecules. For SPh2R molecules, the LDOS at E_f exhibits an oscillatory exponential decay along the molecule, with an average decay constant that depends weakly on the R terminal group. For the mixed aromatic−aliphatic molecules instead, there are large differences in the LDOS at E_f, with $SC4PhCH_3$ showing a much larger LDOS in the proximity of the terminal CH_3 group than $SPhC4CH_3$.

1. Introduction

The challenge of building molecular devices with rectifying, logic, and switching functions has stimulated a huge amount of experimental[1−8] and theoretical[9−13] investigations of systems composed of one (or a few) molecule(s) sandwiched between two metallic electrodes. In particular, systems used for electron tunneling/transport measurements frequently consist of elongated wirelike molecules that are chemisorbed on a metallic substrate through an appropriate headgroup at one end, while the other contact, which may or may not involve chemical bonding, is formed through the tip of a scanning tunneling or conducting tip atomic force microscope.[9,11,14−16] The resulting current depends on many details but primarily on the characteristics of the molecule (e.g., on whether the molecule is conjugated or saturated) and on the contacts (where either chemisorption or physisorption may occur). We shall refer to the systems studied here as "metal/molecule//metal" or "substrate/molecule//tip" molecular junctions to indicate the presence of one chemical and one physical contact and contrast them with the metal/molecule/metal junctions recently studied by our group,[10] in which both ends of the molecule are chemically bound to a metal contact.

In this work we focus on the molecule−tip contact at small bias and study how this is affected by the chemical nature of the molecular terminal group and by the distance of the latter from the tip. We consider metal/molecule//metal junctions formed by conjugated and mixed saturated−conjugated molecules adsorbed on a Au(111) substrate, with the "tip" being represented by another planar Au(111) electrode. We believe the latter to be a reasonable model for tips with radii of curvature (r_C) much larger than the lateral dimensions of the probed molecule(s), as is the case for the tips used in atomic force microscopy (AFM) measurements, which typically have $r_C \approx$ 10−30 nm. Using density functional theory (DFT) calculations with a supercell slab geometry and periodic boundary conditions, we investigate the electronic structure of such junctions, focusing on the local density of states at the Fermi energy E_f (denoted LDOS(E_f) in the following) and the projected density of states (PDOS) at the molecular endgroups. These quantities are known to have a major role in determining the transport properties of the junction at low bias.[17] In particular, by studying the spatial dependence of LDOS(E_f) along the molecular wire, we examine the availability of states spanning the entire molecule and therefore capable to contribute to the low bias conductance. We have recently reported a DFT study of the same type for metal/alkanedithiol/metal junctions in which the molecules are chemically bonded at both ends to two Au(111) electrodes. In that paper, we investigated the dependence of the LDOS(E_f) on the length of the alkane chain and on the distance between the two electrodes. Among other results, we found that when the molecules that fill the gap remain the same but the distance between the electrodes changes (which can be achieved by tilting the molecules at different angles with respect to the surface normal), the LDOS(E_f) remains the same, pointing toward the somewhat surprising result that, in this case, the tunneling current does not depend on the distance between the two electrodes. In this paper, our main purpose is to determine how the LDOS(E_f) and PDOS depend on the chemical identity of the molecular terminal groups and on their distance from the tip. Diphenylthiol (SPh2R) molecules with different terminal groups (R = H, SH, CH_3, or CF_3) as well as mixed phenylthiol-pentane ($SPhC4CH_3$) and butylthiol-toluene ($SC4PhCH_3$) molecules are chosen here as typical examples.

† Part of the special issue "Michael L. Klein Festschrift".

* Author to whom correspondence should be addressed. Phone: (609) 258-3837. Fax: (609) 258-6746. E-mail: aselloni@princeton.edu.

‡ Princeton University.

§ International School for Advanced Studies and Elettra Synchrotron Labs.

10.1021/jp053673i CCC: $33.50
Published on Web 11/02/2005

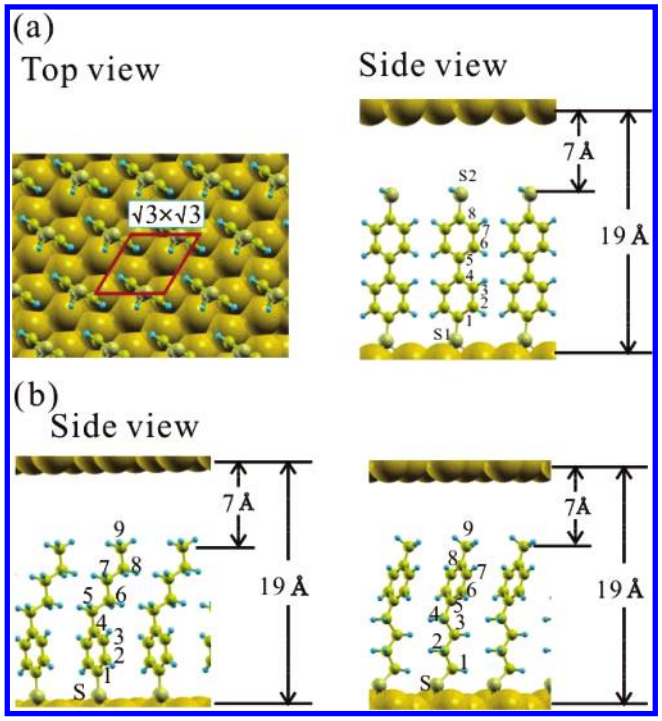

Figure 1. (a) Top and side views of Au(111)/SPh2SH//Au(111). The molecules are chemically bound to one electrode at one end, while the other end has a separation of about 7 Å from the second gold electrode. (b) Optimized geometries of mixed saturated−conjugated molecules sandwiched between two Au(111) surfaces with separation of 19 Å. Au, large yellow spheres; carbon, small yellow spheres; hydrogen, small blue spheres; sulfur, gray spheres.

2. Computational Details and Model Geometry

The calculations have been performed within the plane wave−pseudopotential approach using DFT with the Perdew-Wang 1991 (PW91) exchange−correlation functional.[18,19] Details of the method, such as the pseudopotentials and the energy cutoff for the plane wave basis set, are given in ref 10. The periodic geometry used in our calculations (Figure 1) consists of molecular monolayers sandwiched between slabs of four Au(111) layers. All investigated molecules have a similar length of about 12 Å, and in most calculations there is a distance d_z = 19 Å between the two elecrodes. The molecules have one sulfur headgroup forming a S−Au bond with one of the two Au(111) surfaces, while the other end is separated by a vacuum space of about 7 Å from the second gold surface (Figure 1). A surface $(\sqrt{3} \times \sqrt{3})$ R30 unit cell, with one molecule every three surface Au atoms (corresponding to full monolayer coverage) is used, with a surface nearest-neighbor Au−Au distance of 2.925 Å, as calculated in ref 10. The Brillouin zone has been sampled with eight special *k*-points for the $(\sqrt{3} \times \sqrt{3})$ R30 cell. With the exception of the interelectrode distance that was kept constant, in the geometry optimizations all coordinates were relaxed until each component of the residual force on each atom was smaller than 0.03 eV/Å.

Finally, we like to remind that the PW91 fuctional[18] used in the present study is known to overestimate overlap effects in the regions of small overlap that are important in a few of our calculations as, for example, in the case of the influence of the metal contact proximity on the side of a physical contact. Work is in progress to implement asymptotically corrected functionals in the PWSCF code.[19] When the corrected code is available, it is probable that some quantitative corrections to some of our results may be needed. However, it is unlikely that the qualitative picture may need to be adjusted.

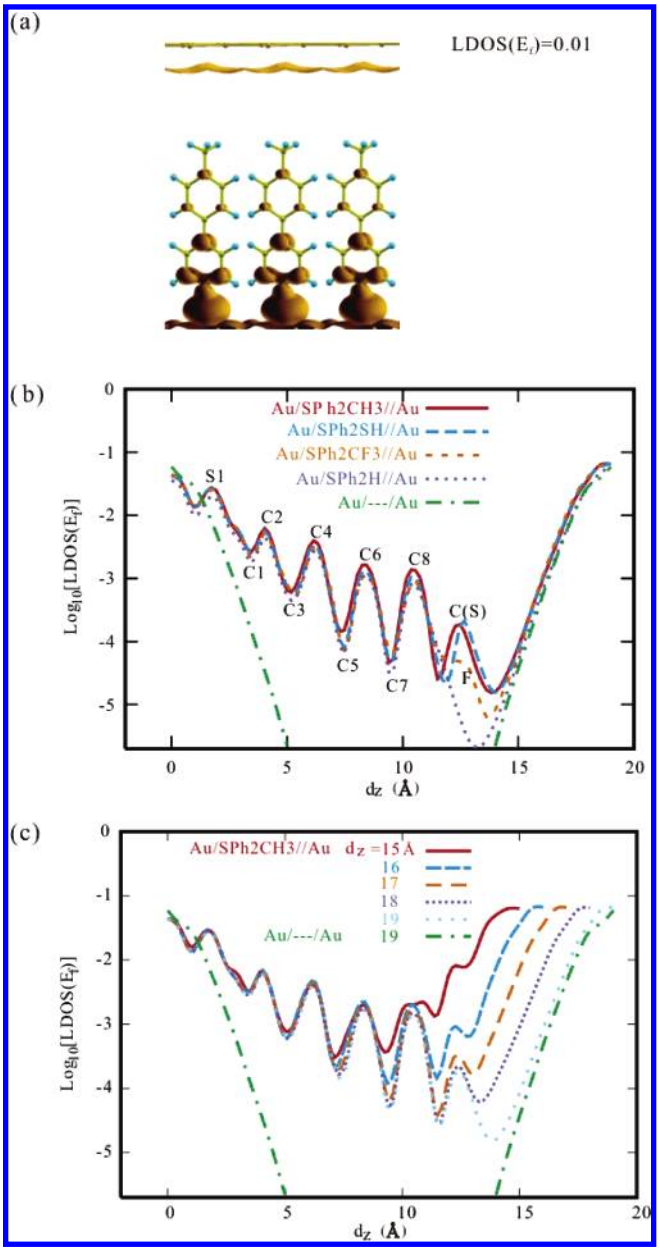

Figure 2. (a) Isosurfaces of LDOS(E_f) for Au(111)/SPh2CH$_3$//Au(111) junctions. The distance between the two electrodes is d_z = 19 Å. (b) Logarithm of the plane-averaged LDOS(E_f) for SPh2R (R = CH$_3$, SH, CF$_3$, or H) sandwiched between two Au(111) surfaces at the distance d_z = 19 Å. The labels of different carbons are given in Figure 1. (c) Logarithm of plane-averaged LDOS(E_f) for Au(111)/SPh2CH$_3$//Au(111) with separations of 19, 18, 17, 16, and 15 Å between the two gold electrodes. For comparison, the plane-averaged LDOS(E_f) values for the bare Au surfaces are also given.

3. Results

3.1. Local Density of States at E_f. *3.1 1. Au(111)/SPh2R//Au(111), R = CH$_3$, CF$_3$, SH, or H.* The optimized structure of the junction formed by SPh2R with R = CH$_3$ is shown in Figure 1a. At monolayer coverage, the diphenyl-thiolate molecule is adsorbed almost vertically on the Au(111) substrate, with the sulfur atom at the bridge site slightly shifted toward the face-centered cubic (fcc) hollow site, and the calculated S−Au bond length is about 2.49 Å. These structural results agree well with DFT calculations for benzenethiol adsorption on Au(111)[20] as well as with recent X-ray diffraction results,[21] which found the tilt angle to be less than 19°.

Given the important role of the LDOS(E_f) in the transport properties of the molecular junction at low bias,[17] in Figure 2a

we present three-dimensional LDOS(E_f) isosurfaces for the representative case of the junction formed by the $SPh2CH_3$ molecule, while in Figure 2b we plot the plane-averaged LDOS(E_f) as a function of the distance along the surface normal (d_z) direction for the different R terminations. We can see that LDOS(E_f) exhibits a complex behavior in which oscillations are superimposed to an exponential decay. The oscillations indicate a resonant behavior of the charge distribution in the phenyl rings. Such oscillations are not observed in the density of states of the isolated diphenyl molecules but originate in part from a polarization effect and, as we shall see later, from the surface to molecule charge transfer through the sulfur headgroup. The exponential decay of the LDOS(E_f) along the molecular junction yields an average decay constant β between 0.38 and 0.43 $Å^{-1}$, very similar for all the investigated terminal groups. As a comparison, the decay constant that we find for the bare gold surface is $\beta_{Au} \approx 2.4$ $Å^{-1}$, which yields $\varphi_{Au} = (\beta_{Au})^2/8 \approx 5.4$ eV for the work function, in good agreement with the experimental value of 5.1−5.3 eV. The corresponding "effective tunneling barriers" $\varphi = (\beta)^2/8$ for the molecular junctions vary in a narrow energy range, from 0.14 eV, for R = SH and CH_3, to 0.18 eV, for R = H and CF_3. These effective barriers are usually associated with the distance of the molecular highest occupied molecular orbital (HOMO) or lowest unoccupied molecular orbital (LUMO) from the metal Fermi energy.[22] However, this assignment is not evident from the detailed analysis of the projected density of states for the molecular junction (see below, section 3.2, and Figures 4−6).

Figure 2c shows how the plane-averaged LDOS(E_f) depends on the distance between the molecular terminal group and the tip electrode. We consider the $SPh2CH_3$ molecule as a prototype and progressively reduce its distance to the tip from ∼7 to 3 Å by steps of about 1 Å. When the distance is decreased, the LDOS(E_f) in proximity of the CH_3 endgroup increases dramatically. At some point, the average decay constant β is no longer well-defined, suggesting a transition from tunneling to point contact regime.[23]

3.1.2. Au/SPhC4CH₃//Au and Au/SC4PhCH₃//Au. We now consider Au/molecule//Au junctions formed by molecules that contain both a conjugated phenyl ring and a saturated alkane (butane) chain and where either the phenylthiol (case A) or the butanethiol (case B) end are chemically bound to electrode I. In both cases the terminal group is a CH_3 group separated by about 7 Å from the second gold electrode (Figure 1b). In the optimized structure for case A, the phenylthiol adsorbs vertically at the bridge (slightly shifted to fcc) site, and the averaged S−Au bond length is 2.52 Å. Above the phenylthiol, the tilt angle of the alkane chain with respect to the surface normal is about 29°. In case B, butanethiol adsorbs at the bridge site, the mixed molecule has a tilt angle of 13° respect to the surface normal, and the S−Au bond length is 2.46 Å.

In Figure 3, we show isosurfaces of the LDOS(E_f) as well as the plane-averaged LDOS(E_f) along the surface normal direction for the two contact cases considered. It is evident that the differences between the two molecules are quite large. When the chemical contact with the substrate occurs via the aromatic part of the molecule (case A), the LDOS(E_f) decays exponentially along the molecule, the averaged decay constant is rather large (about 0.79 $Å^{-1}$), and the oscillatory behavior is similar to that of the LDOS(E_f) for Au/SPh2R//Au as shown in Figure 2. For case B, instead, after an initial exponential decay along the saturated chain, the LDOS(E_f) increases and remains always much larger than that in case A, resulting in a very small

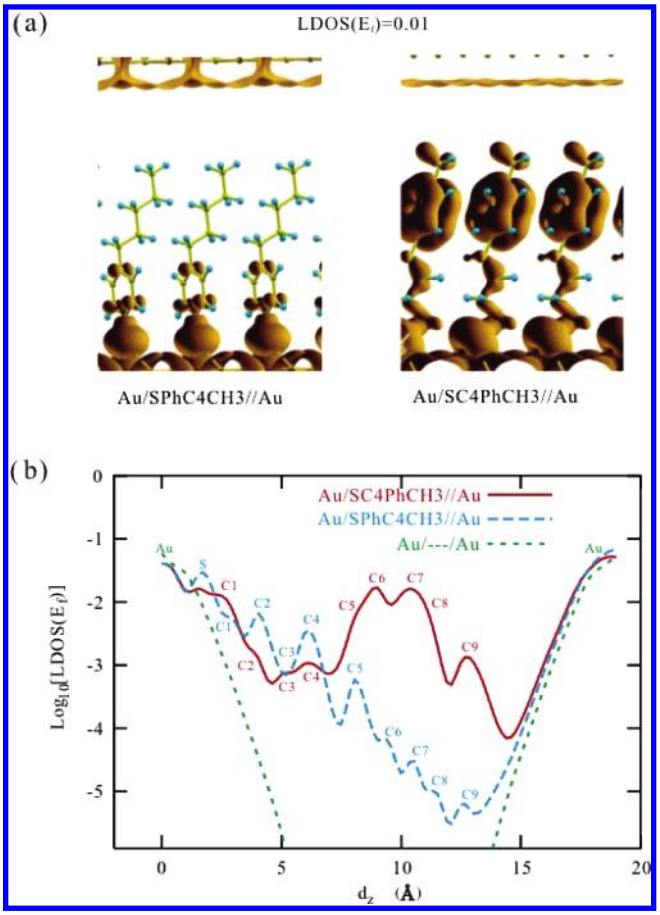

Figure 3. Isosurfaces of the LDOS(E_f) (upper panel) and logarithm of the plane-averaged LDOS(E_f) along the d_z direction (lower panel) for the molecular junctions formed by $SPhC4CH_3$ and $SC4PhCH_3$. sandwiched between two Au(111) surfaces at a distance of 19 Å. The labels of different carbons are given in Figure 1. Long-dashed line, case A (benzenethiol contact); full line, case B (butylthiol contact); short-dashed line, bare gold surfaces.

averaged decay constant along the junction. A qualitative explanation of this behavior is given in the next section.

3.2. Projected Density of States. *3.2.1. Au(111)/SPh2R//Au(111), R = CH₃, CF₃, SH, or H.* Figure 2b shows that while chemically different terminal groups have little influence on the average decay constant β significant differences in the LDOS(E_f) occur in proximity to the terminal groups themselves. For instance, the averaged LDOS(E_f) at the SH and CH_3 terminals are remarkably larger than those at the CF_3 and H terminals. These differences are illustrated in more detail in Figure 4, which shows the PDOS for the different R terminal groups of the diphenyl SPh2R molecules, at two representative values, $d = 3$ and 7 Å, of the R−tip distance. Due to the stronger tip−molecule electronic overlap, all PDOS features appear broader at the shorter, $d = 3$ Å, distance. Incidentally, the PDOS for the CH_3 and CF_3 terminals in Figure 4b show some interesting similarities with experimental (I/V)(dI/dV) curves for CH_3- and CF_3-terminated decanethiol monolayers on Au(111) obtained in recent scanning tunneling microscopy (STM) measurements.[14] Analysis of these data is currently in progress in our group.

It is also interesting to consider how the electronic structure changes along the molecular junction. To this end, in Figure 5 we show the density of states projected onto the sulfur, phenyl, and terminal subgroups of Au/$SPh2CH_3$//Au and compare these to the corresponding PDOS of the isolated $SPh2CH_3$ radical and the bare Au(111) surface. The energy levels of Au/$SPh2CH_3$//Au and of the bare surface have been aligned

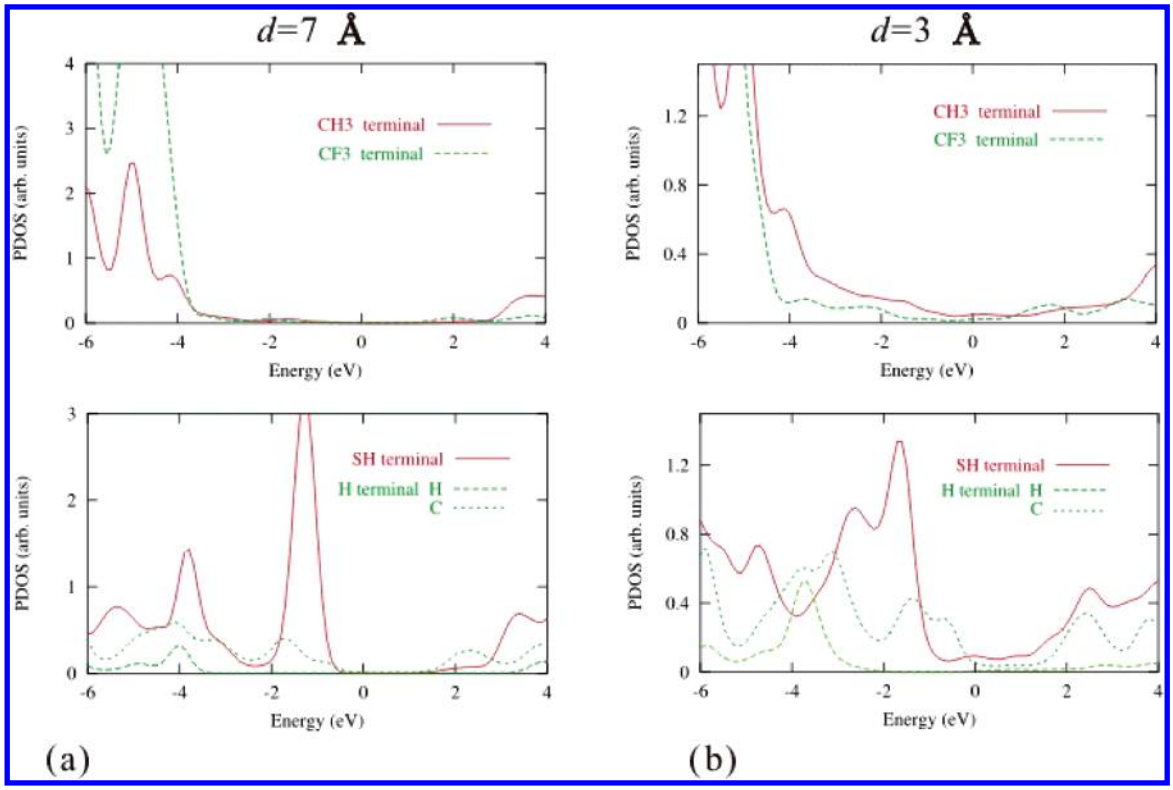

Figure 4. Projected densities of states on the molecular terminal R (R = CH_3, SH, CF_3, or H) for Au(111)/SPh2R//Au(111). Two different distances of the molecular terminal to the tip electrode are considered.

assuming the same Fermi level, while the energy levels of the isolated $SPh2CH_3$ radical have been aligned by taking the vacuum level as the reference energy. Figure 5 shows that the PDOS onto the sulfur atom and the phenyl rings are broadened due to hybridization between the molecular orbitals and the bands of the gold surface and acquire small tails across E_f. We can also see in Figure 5 that the LUMO of the isolated $SPh2CH_3$ radical (shown in one of the insets) falls about 1 eV below the Fermi energy of the bare Au(111) surface. Thus, some charge is transferred from the surface to the molecule upon adsorption, which, in turn, causes an upward shift of the energies of the molecular orbitals. In particular, the second inset of Figure 5 shows a state of the interacting Au/$SPh2CH_3$//Au system at ~0.5 eV below E_f, which clearly originates from the coupling of the molecular LUMO to the gold surface. The charge transfer that we have here illustrated for $SPh2CH_3$ is not unique to this molecule but occurs for the other SPh2R molecules as well and was also observed for (di)phenyldithiol molecules sandwiched between two Au(111) surfaces,[10] suggesting that this may be a general effect for conjugate thiol molecules chemisorbed on gold surfaces through a S−Au bond.

3.2.2. Au/SPhC4CH₃//Au versus Au/SC4PhCH₃//Au.. In Figure 6 we show the computed PDOS for the two junctions. We first notice that the position of the sulfur peak, about 1 eV below E_f, is practically identical in the two cases and also similar to the position of the S peak for SPh2R (Figure 5), suggesting that the electronic structure of the interface is largely determined by the characteristics of the S−Au bond. From Figure 6, it can be also seen that the highest occupied levels of the carbons in the phenyl ring for case B, where this ring is substantially decoupled from the sulfur headgroup and thus from the surface, are just below E_f (Figure 6c_1), whereas they lie more than 2 eV below E_f in case A, where the phenyl ring is strongly coupled to the surface through the S headgroup (Figure 6b). Thus the PDOS near E_f for the CH_3 terminal is much larger for case B (compare Figure 6d and 6d_1), and correspondingly, also the low

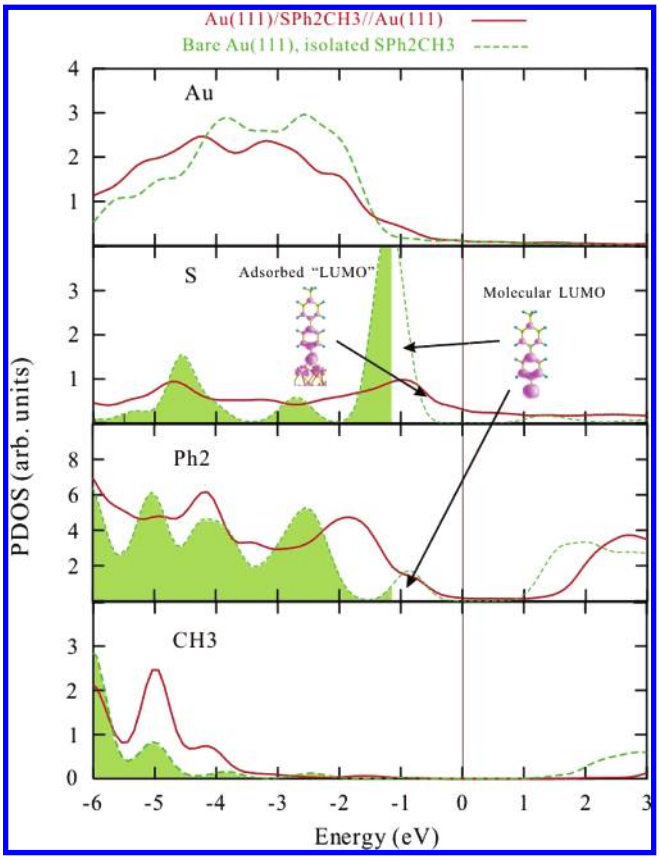

Figure 5. PDOS for Au(111)/$SPh2CH_3$//Au(111) compared to the PDOS of the isolated $SPh2CH_3$ radical and that of the bare Au(111) surface. The green areas in the PDOS for the isolated $SPh2CH_3$ radical indicate the filled states. The distance between the two Au(111) electrodes is 19 Å. The energy zero corresponds to the Fermi energy. The insets show isosurfaces of the LUMO for the isolated $SPh2CH_3$ radical (molecular LUMO) and of the state resulting from the coupling of this orbital with the states of the gold surface (chemisorbed LUMO).

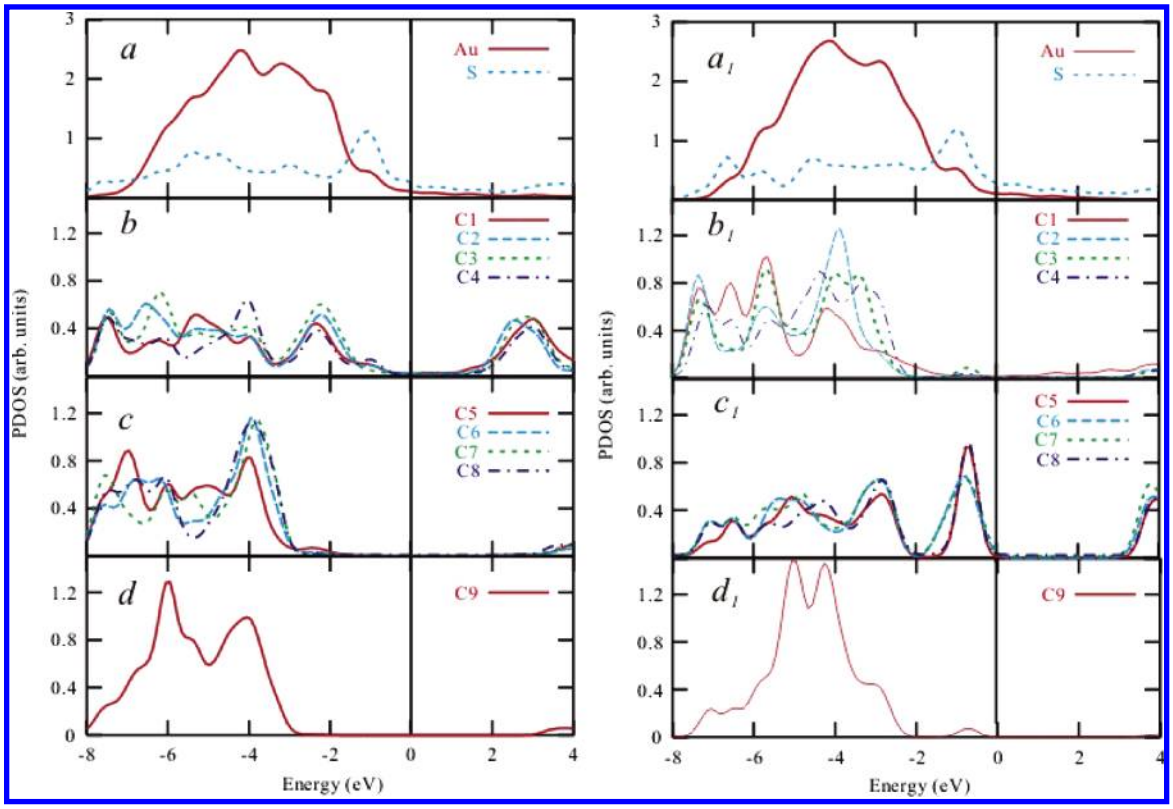

Figure 6. PDOS of the Au(111)/mixed molecule//Au(111) system. Left panel, $SPhC4CH_3$ (case A); right panel, $SC4PhCH_3$ (case B). The distance between the two Au(111) electrodes is 19 Å. The energy zero corresponds to E_f.

bias tunneling probability is likely to be higher in case B. This somewhat surprising result is reminiscent of the counterintuitive effect found in ref 24, where upon decoupling one of the two S atoms of the SPhS moiety from its gold electrode the HOMO of the phenyl ring appeared to move up to a closer alignment with the metal Fermi level, thus increasing the transmission coefficient at the Fermi level and correspondingly the low-bias tunneling conductance.

3.2.3. Charge Transfers and Decay Constant.. An interesting question to address is the relationship between the surface to molecule charge transfer (CT) and the average decay constant, β, of the LDOS(E_f). We evaluate the surface to molecule CT by integrating the PDOS of the adsorbed molecule up to E_f . In this way, for SPh2CH3 we calculate a CT of about 0.45*e*, comprising 0.17*e* to the sulfur headgroup and 0.28*e* to Ph2CH3 (0.14*e* and 0.12*e* to the first and second phenyl group, respectively). Similarly, for SPhC4CH3 we obtain a CT of about 0.31*e* (0.20*e* to sulfur and 0.11*e* to the adjacent Ph unit), whereas the CT is smaller, 0.23*e*, for SC4PhCH3 (0.20*e* to sulfur, and 0.03*e* to the adjacent C4 unit). Apparently, the CT always includes a contribution of approximately 0.20*e* to the S headgroup, with an additional contribution that varies depending on whether the sulfur atom is followed by a conjugated or saturated unit; in the former case the computed CT is ~0.12*e* per phenyl group, whereas saturated alkane chains accept only a very small charge transfer on the order of $10^{-2}e$. This is confirmed by a calculation of the gold surface to molecule CT for purely saturated alkanethiolate SC8 molecules, which yields a value of about 0.23*e* (0.20*e* to S and 0.03*e* to C8). Incidentally, we notice that this value is in good agreement with a previous theoretical study based on a Mulliken population analysis,[25] whereas a different type of estimate, based on work-function changes induced by methylthiolate adsorbates, indicates a smaller or negligible CT.[26]

While our computed CT for SC8 is the same as that found for SC4PhCH3, the average decay constant β for alkanethiols, 0.8−0.9 $Å^{-1}$,[10−12,15,16] is quite different (much larger) with respect to the average decay of SC4PhCH3 in Figure 3b. This indicates that the average β is not so much affected by the interface CT as by the conjugation versus saturation properties of the whole molecule. This conclusion is also supported by a comparison of the CTs and decay constants for SC8 molecules on two different metallic surfaces, namely, Au(111) and Ag(111). In agreement with experiment,[27] the computed β is the same for the two surfaces, despite the fact that for Ag(111)/SC8//Ag(111) the CT is much larger, 0.38*e* (0.35*e* to sulfur and 0.03*e* to C8), against the CT of 0.23*e* for Au(111)/SC8//Au(111). Notice, however, that the larger CT of Ag(111) with respect to Au(111) only concerns the S headgroup, i.e., is localized at the interface. The CT to C8 has the same small value, 0.03*e*, on both surfaces, in line with their identical and large β values.

4. Summary and Conclusions

In this paper we have presented a DFT-based computational study of the electronic structure of substrate/molecule//tip junctions in which both the substrate and the tip consist of a Au(111) surface. We have considered diphenylthiol molecules with various terminal endgroups as well as mixed aromatic−aliphatic molecules consisting of one phenyl ring and one alkane chain. For the diphenylthiol molecules, we found that the spatial dependence of the local density of states at the Fermi energy, LDOS(E_f), is characterized by an oscillatory (resonance) behavior superimposed with an exponential decay along the molecule. The average decay constant β varies in a narrow range, between 0.38 and 0.43 $Å^{-1}$, for the different terminal endgroups. By contrast, the energy-dependent projected density of states shows specific features for each terminal group. These

different features should show up in the experimental $I-V$ characteristics at low bias, as recently observed for decanethiols with CH_3 and CF_3 terminal groups.[14]

For the mixed conjugated−saturated molecule, we found large differences in the electronic properties depending on whether the chemical contact is through phenylthiol or the alkanethiol chain, $SC4PhCH_3$ showing a much larger LDOS(E_f) in the proximity of the terminal CH_3 group than that of $SPhC4CH_3$. Since the LDOS(E_f) is related to the zero-bias current, for the mixed molecule the chemical contact through the alkanethiol end should lead to higher currents.

Finally, from our results we conclude that electron tunneling through metal/molecule//metal junctions cannot be easily predicted using intuitive arguments based on the chemical nature of the molecule that spans the gap; detailed calculations may be necessary even for qualitative predictions.

Acknowledgment. Calculations were performed on the IBM-SP3 computer of the Keck Computational Materials Science Laboratory in Princeton. This work was partially supported by the National Science Foundation through Grant No. DMR02-13706 to the MRSEC Princeton Center for Complex Materials.

References and Notes

(1) Selzer, Y.; Salomon, A.; Cahen, D. *J. Phys. Chem. B* **2002**, *106*, 10432−10439.

(2) Liu, Y.-J.; Yu, H.-Z. *ChemPhysChem* **2003**, *4*, 335−342.

(3) Metzger R. M. *Chem. Rev.* **2003**, *103*, 3803−3834.

(4) Donhauser, Z. J.; Mantooth, B. A.; Kelly, K. F.; Bumm, L. A.; Monnell, J. D.; Stapleton, J. J.; Price, D. W., Jr.; Rawlett, A. M.; Allara, D. L.; Tour, J. M.; Weiss, P. S. *Science* **2001**, *292*, 2303−2307.

(5) Ramachandran, G. K.; Hopson, T. J.; Rawlett, A. M.; Nagahara, L. A.; Primak, A.; Lindsay, S. M. *Science* **2003**, *300*, 1413−1416.

(6) Lau, C. N.; Stewart, D. R.; Williams, R. S.; Bockrath, M. *Nano Lett.* **2004**, *4*, 569−572.

(7) Wang, W.; Lee, T.; Reed, M. A. *J. Phys. Chem. B*, **2004**, *108*, 18398−18407.

(8) Nitzan, A.; Ratner, M. A. *Science* **2003**, *300*, 1384−1389.

(9) Joachim, C.; Gimzewski, J. K.; Aviram, A. *Nature* **2000**, *408*, 541−548.

(10) (a) Piccinin, S.; Selloni, A.; Scandolo, S.; Car, R.; Scoles, G. *J. Chem. Phys.* **2003**, *119*, 6729. (b) Sun, Q.; Selloni, A.; Scoles, G. *ChemPhysChem* **2005**, *6*, 1906−1910.

(11) Xue, Y.; Datta, S.; Ratner, M. A. *J. Chem. Phys.* **2001**, *115*, 4292−4299.

(12) Tomfohr, J. K.; Sankey, O. F. *Phys. Rev. B* **2002**, *65*, 245105−12.

(13) Gebauer, R.; Car, R. *Phys. Rev. Lett.* **2004**, *93*, 160404−4.

(14) Pflaum, J.; Bracco, G.; Schreiber, F.; Colorado, R., Jr.; Shmakova, O. E.; Lee, T. R.; Scoles, G.; Kahn, A. *Surf. Sci.* **2002**, *498*, 89−104.

(15) Wold, D. J.; Haag, R.; Rampi, M. A.; Frisbie, C. D. *J. Phys. Chem. B.* **2002**, *106*, 2813−2816.

(16) Beebe, J. M.; Engelkes, V. B.; Miller, L. L.; Frisbie, C. D. *J. Am. Chem. Soc.* **2002**, *124*, 11268−11269.

(17) (a) Tersoff, J.; Hamann, D. R. *Phys. Rev. Lett.* **1983**, *50*, 1998−2001. (b) Lang, N. D. *Phys. Rev. B* **1986**, *34*, 5947−5950. (c) Datta, S. *Electronic Transport in Mesoscopic Systems*; Cambridge University Press: Cambridge, U. K., 1995; Chapter 3.

(18) Perdew, J. P.; Chevary, J. A.; Vosko, S. H.; Jackson, K. A.; Singh, D. J.; Fiolhais, C. *Phys. Rev. B* **1992**, *46*, 6671.

(19) We used the PWSCF code by S. Baroni, S. De Gironcoli, A. Dal Corso, and P. Giannozzi, available at http://www.pwscf.org.

(20) Nara, J.; Higai, S.; Morikawa, Y.; Ohno, T. *J. Chem. Phys.* **2004**, *120*, 6705−6711.

(21) Leung, T. Y. B.; Schwartz, P.; Scoles, G.; Schreiber, F.; Ulman, A. *Surf. Sci.* **2000**, *458*, 34−52.

(22) Salomon, A.; Cahen, D.; Lindsay, S.; Tomfohr, J.; Engelkes, V. B.; Frisbie, C. D. *Adv. Mater.* **2003**, *15*, 1881−1890.

(23) (a) Lang, N. D. *Phys. Rev. B* **1988**, *37*, 10395−10398. (b) Ciraci, S.; Tekman, E. *Phys. Rev. B* **1989**, *40*, 11969−11972. (c) Ciraci, S. In *Scanning Tunneling Microscopy III*; Wiesendanger, R., Guenteroth, H.-J., Eds.; Springer-Verlag: Berlin, 1996; pp 182−197.

(24) Xue, Y.; Ratner, M. A. *Phys. Rev. B* **2003**, *68*, 115407.

(25) Grönbeck, H.; Curioni, A.; Andreoni, W. *J. Am. Chem. Soc.* **2000**, *122*, 3839−3842.

(26) De Renzi, V.; Rousseau, R.; Marchetto, D.; Biagi, R.; Scandolo, S.; del Pennino, U. *Phys. Rev. Lett.* **2005**, *95*, 046904.

(27) Engelkes, V. B.; Beebe, J. M.; Frisbie, C. D. *J. Am. Chem. Soc.* **2004**, *126*, 14287−14296.